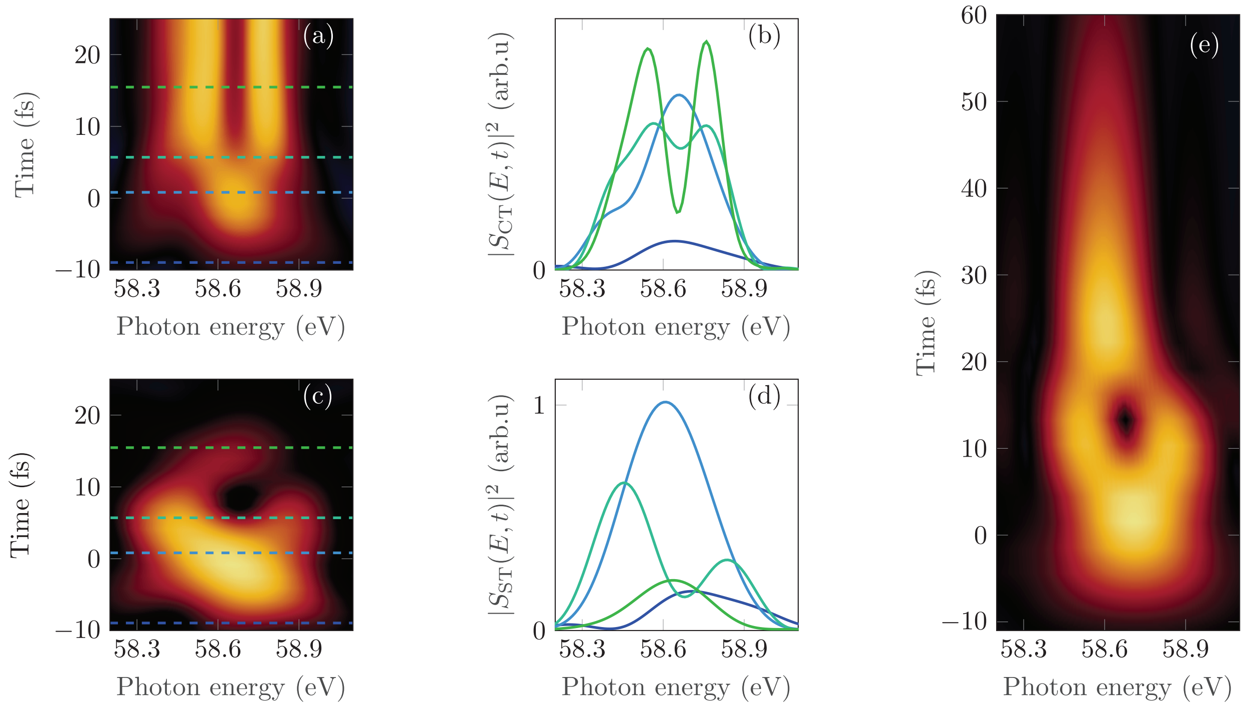

Figure 7. (a) Representation of $|S_{\rm C}|^2$ in colors, as a function of E_f and t. (b) Lineouts of $|S_{\rm C}|^2$ at the times indicated by the dashed lines in (a). (c) Representation of $|S_{\rm ST}|^2$ in colors, as a function of E_f and t. (d) Lineouts of $|S_{\rm ST}|^2$ at the times indicated by the dashed lines in (c). (e) Representation of $|S_{\rm ST}|^2$ in colors, as a function of E_f and t using simulated data for a 10 nm broad IR pulse.

and can be seen as the Fourier transform of the auto-correlation function of the EWP. Additionally, one of the properties of this distribution is that the projections along the time (respectively frequency) axes (referred to as *marginals* in the literature) generates the spectral (respectively temporal) intensity of the wave packet: $\int W(E_{\rm f},t){\rm d}t = |A_{\rm n+1}(E_{\rm f})|^2$ and $2\pi\int W(E_{\rm f},t){\rm d}E_{\rm f} = |\tilde{A}_{\rm n+1}(t)|^2$. Finally, an interesting feature of this representation is that it is not a positive distribution. In the WD of coherent multicomponent signals, the different components interfere with each other and the distribution can take negative values.

Figure 8(a) shows the experimental Wigner distribution (WD) of the two-photon EWP emitted through the sp2$^+$ resonance. The spectrally large peak centered at $t = 0$ fs represents, like for the STFT, the direct ionization path. The temporally long and spectrally narrow feature centered at $E_{\rm f} = 58.6$ eV describes the decay of the sp2$^+$ state. Because these two processes have such distinct spectral-temporal representations, it is very easy to disentangle the direct ionization to the continuum states from the autoionization through the sp2$^+$ state. The negative peak and the shoulder between $E_{\rm f} = 58.7$ eV and $E_{\rm f} = 58.8$ eV represent the interferences between the two ionization paths. These results agree very well with the theoretical calculations as shown in figure 8(b). These interference effects provide information on the correlation between the direct and resonant ionization amplitudes. In our experimental conditions, the IR pulses were too short to allow a complete visualization of these correlation effects. In figure 8(c) we show the simulation of the WD that would be obtained using the same XUV pulses but spectrally-narrower IR pulses of 10 nm bandwidth corresponding to a pulse duration of roughly 100 fs. Very clear oscillations appear between 58.6 and 58.9 eV compared to the simulation in the experimental conditions. These oscillations are characterized by a frequency that increases linearly with the detuning and an amplitude that is damped as a function of time.

5.3. Analytical Wigner distribution

In this section we derive analytically the expression of the Wigner distribution for the complex Fano amplitude (equation 1). We first take the Fourier transform as in [25, 16]:

$$\tilde{R}(t) = \delta(t) - i\frac{\Gamma}{2\hbar}(q-i)\,{\rm e}^{-(iE_\Phi/\hbar+\Gamma/2\hbar)t}\,\Theta(t) \qquad (12)$$

The Wigner distribution can be written as the sum of three terms, $W(E_{\rm f},t) = W_D + W_I + 2{\rm Re}\,(W_{ID})$, which